Electronic Supplementary Material (ESI) for Journal of Materials Chemistry C

Supporting information

In situ purification to eliminate the influence of impurities in solution-processed organic crystals for transistor arrays

Yun Li,[a,b,*] Chuan Liu,[a,*] Micael V. Lee,[a] Yong Xu,[a] Xu Wang,[a] Yi Shi[b] and Kazuhito Tsukagoshi[a]

[a] *International Center for Materials Nanoarchitectonics (WPI-MANA), National Institute for Materials Science (NIMS), Tsukuba, Ibaraki 305-0044, Japan.*

E-mail: TSUKAGOSHI.Kazuhito@nims.go.jp

[b] *School of Electronic Science and Engineering, Nanjing University, Nanjing 210093, People's Republic of China.*

E-mail: yshi@nju.edu.cn

[*] *These authors contributed equally to this work.*

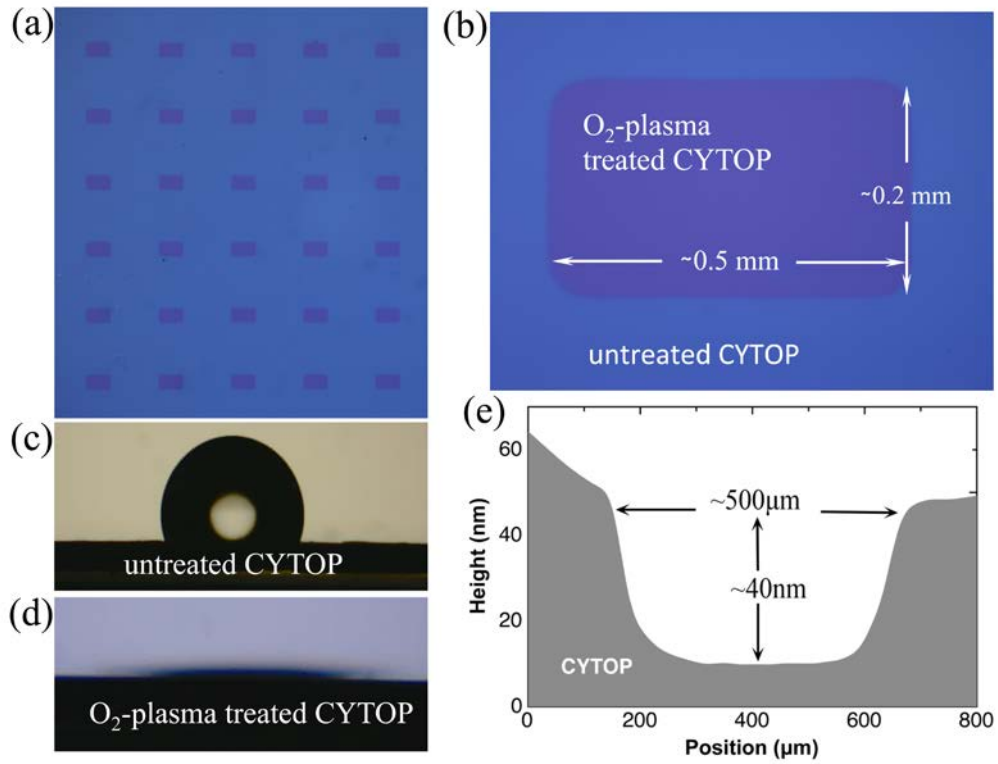

Figure S1. (a) (b) Microscopy images of the CYTOP film with patterned arrays after the O_2-plasma treatment. Water contact angles of an untreated (c) and plasma-treated (d) CYTOP surface. (e) Cross-sectional profile of a patterned region.

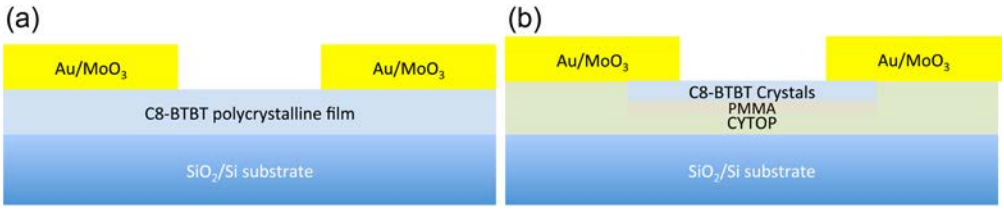

Figure S2. Schematics of the device structures for C8-BTBT polycrystalline thin films from spin-coating bare C8-BTBT solutions (a) and for patterned C8-BTBT crystals using direct spin-coating from C8-BTBT/PMMA blends (b).

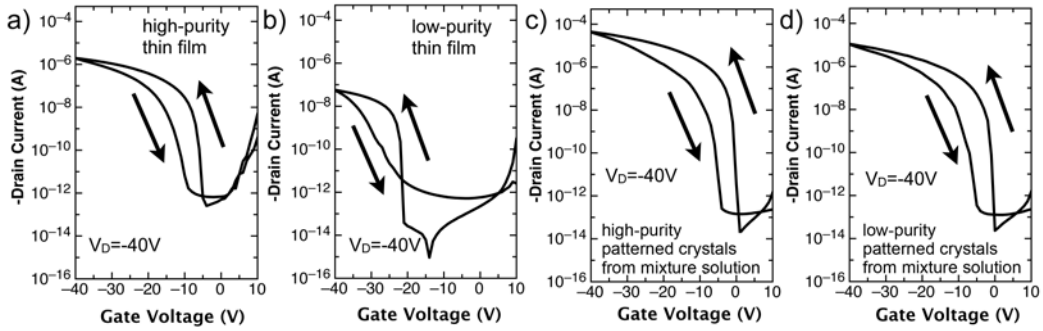

Figure S3. Typical transfers curves for high- (a) and low-purity (b) polycrystalline thin films of C8-BTBT. Obvious increase in hysteresis can be observed. Meanwhile, the hysteresis in the devices based on high- (c) and low-purity (d) patterned C8-BTBT crystals was similar with each other.

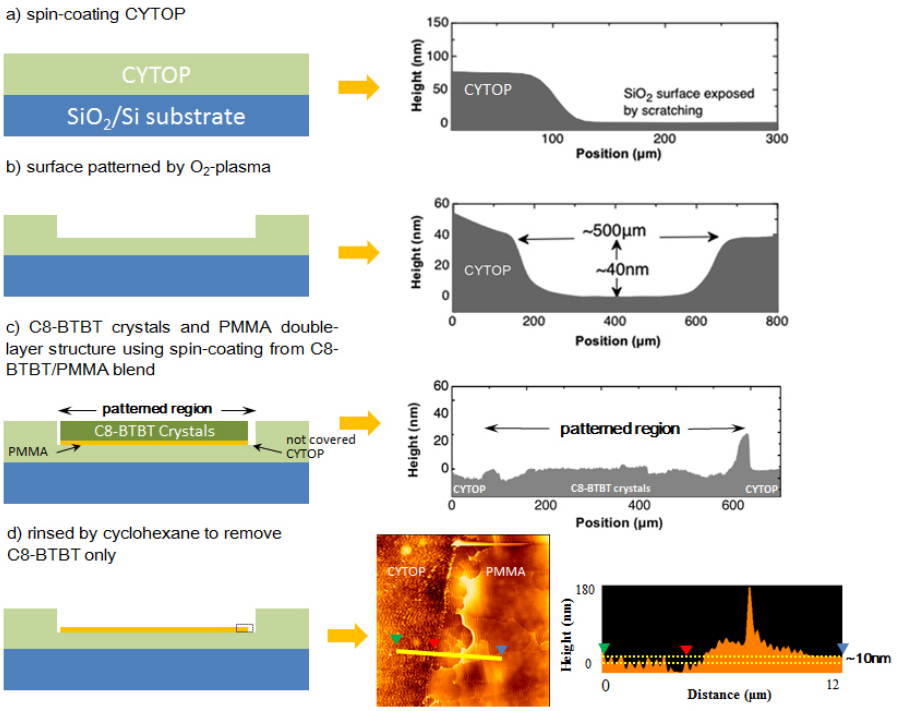

Figure S4. (a) Schematic illustration of the process of spin-coating a CYTOP layer (left); the cross-sectional profile of a CYTOP layer partly exposed by scratching, indicating a ~75 nm thick CYTOP (right). (b) The process of oxygen-plasma treatment that results in a patterned CYTOP layer (left); the cross-sectional profile of a patterned region of CYTOP, showing the depth of ~40 nm (right). (c) The process of spin-coating from C8-BTBT/PMMA blends that produces C8-BTBT plate-like crystals and PMMA double-layer structure (the gap between the double-layer structures and the CYTOP edge is the CYTOP region with no coverage of C8-BTBT or PMMA) (left); the cross-sectional profile of a patterned region with C8-BTBT plate-crystals (right). (d) In order to measure the PMMA thickness underneath the C8-BTBT crystals, we rinsed the sample by cyclohexane to remove C8-BTBT only (left); Atomic force microscopy (AFM) image (20 μm ×20 μm) of the edge between CYTOP and PMMA (highlighted by the black dotted square in the schematic illustration in Figure R1d) (middle); The AFM profile taken across the line in the AFM image, showing a very thin PMMA layer with the thickness of ~10nm (right).

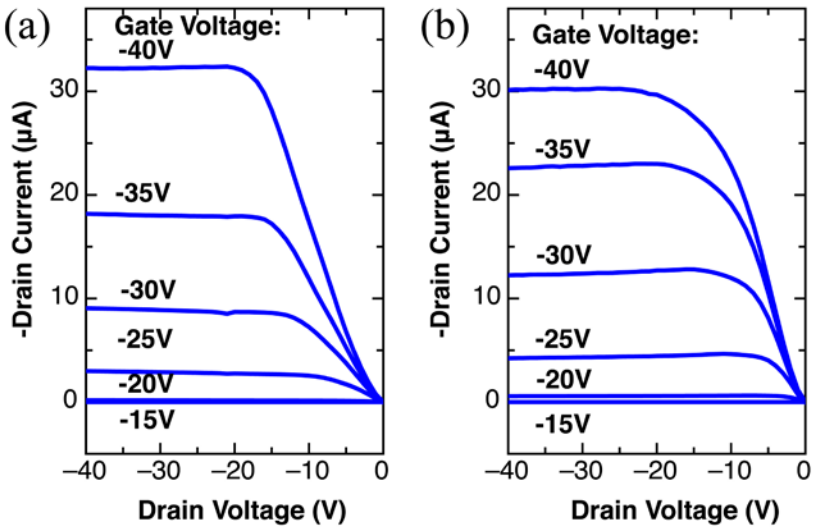

Figure S5. Output curves of the FET arrays with patterned C8-BTBT plate-like crystals spin-coated from high- (a) and low-purity (b) C8-BTBT solutions blended with PMMA.

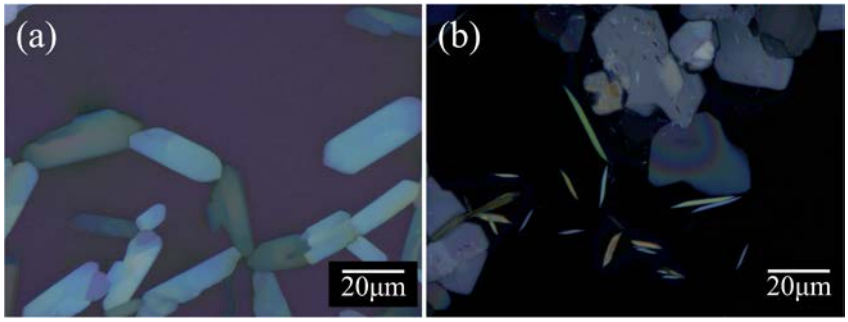

Figure S6. Organic crystals grown from high- (a) and low-purity (b) C8-BTBT using solvent-vapor annealing.

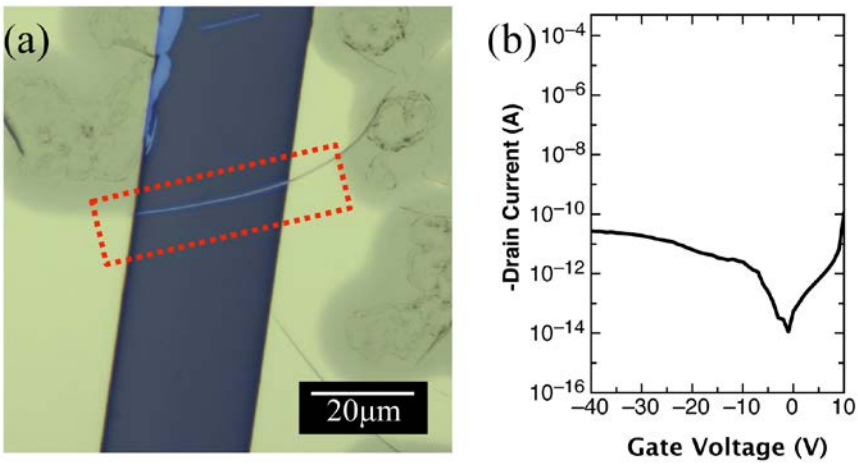

Figure S7. (a) Microscopy image of an isolated needle-like crystal of impurity (highlighted by red-dotted square) bridging the source and drain electrodes. (b) Electrical characteristics of the impurity crystal, which exhibited low electrical conduction and almost no transistor behavior.

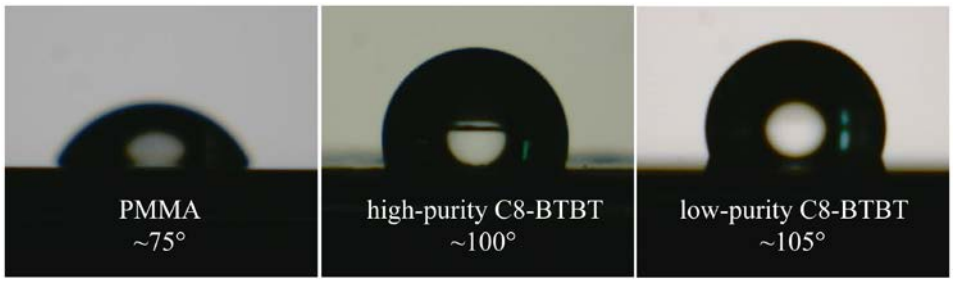

Figure S8. Water contact angles of thin films of bare PMMA (left), high-purity (middle) and low-purity (right) C8-BTBT. The PMMA surface has the smallest contact angle, which indicates that PMMA has a higher surface energy than C8-BTBT and impurity molecules.